

## UC Irvine

### UC Irvine Previously Published Works

#### Title

Effects of N-Terminal Residues on the Assembly of Constrained  $\beta$ -Hairpin Peptides Derived from A $\beta$ .

#### Permalink

<https://escholarship.org/uc/item/7ws9n3wc>

#### Journal

Journal of the American Chemical Society, 142(26)

#### Authors

Samdin, Tuan  
Wierzbicki, Michal  
Kreutzer, Adam  
[et al.](#)

#### Publication Date

2020-07-01

#### DOI

10.1021/jacs.0c05186

Peer reviewed



Published in final edited form as:

*J Am Chem Soc.* 2020 July 01; 142(26): 11593–11601. doi:10.1021/jacs.0c05186.

## Effects of *N*-Terminal Residues on the Assembly of Constrained $\beta$ -Hairpin Peptides Derived from $A\beta$

Tuan D. Samdin<sup>a</sup>, Michał Wierzbicki<sup>a</sup>, Adam G. Kreutzer<sup>a</sup>, William J. Howitz<sup>a</sup>, Mike Valenzuela<sup>a</sup>, Alberto Smith<sup>a</sup>, Victoria Sahrai<sup>a</sup>, Nicholas L. Truex<sup>a</sup>, Matthew Klun<sup>a</sup>, James S. Nowick<sup>a,b</sup>

<sup>a</sup>Department of Chemistry, University of California, Irvine, California 92697-2025, United States

<sup>b</sup>Department of Pharmaceutical Sciences, University of California, Irvine Irvine, California 92697-2025, United States

### Abstract

This paper describes the synthesis, solution-phase biophysical studies, and X-ray crystallographic structures of hexamers formed by macrocyclic  $\beta$ -hairpin peptides derived from the central and *C*-terminal regions of  $A\beta$ , which bear “tails” derived from the *N*-terminus of  $A\beta$ . Soluble oligomers of the  $\beta$ -amyloid peptide,  $A\beta$ , are thought to be the synaptotoxic species responsible for neurodegeneration in Alzheimer’s disease. Over the last 20 years, evidence has accumulated that implicates the *N*-terminus of  $A\beta$  as a region that may initiate the formation of damaging oligomeric species. Our laboratory has previously studied macrocyclic  $\beta$ -hairpin peptides derived from  $A\beta_{16-22}$  and  $A\beta_{30-36}$ , capable of forming hexamers that can be observed by X-ray crystallography and SDS-PAGE. To better mimic oligomers of full length  $A\beta$ , we use an orthogonal protecting group strategy during the synthesis to append residues from  $A\beta_{1-14}$  to the parent macrocyclic  $\beta$ -hairpin peptide **1**, which comprises  $A\beta_{16-22}$  and  $A\beta_{30-36}$ . The *N*-terminally extended peptides **N+1**, **N+2**, **N+4**, **N+6**, **N+8**, **N+10**, **N+12**, and **N+14** assemble to form dimers, trimers, and hexamers in solution-phase studies. X-ray crystallography reveals that peptide **N+1** assembles to form a hexamer that is composed of dimers and trimers. These observations are consistent with a model in which the assembly of  $A\beta$  oligomers is driven by hydrogen bonding and hydrophobic packing of the residues from the central and *C*-terminal regions, with the *N*-terminus of  $A\beta$  accommodated by the oligomers as an unstructured tail.

### Graphical abstract

**Corresponding Author** jsnowick@uci.edu.

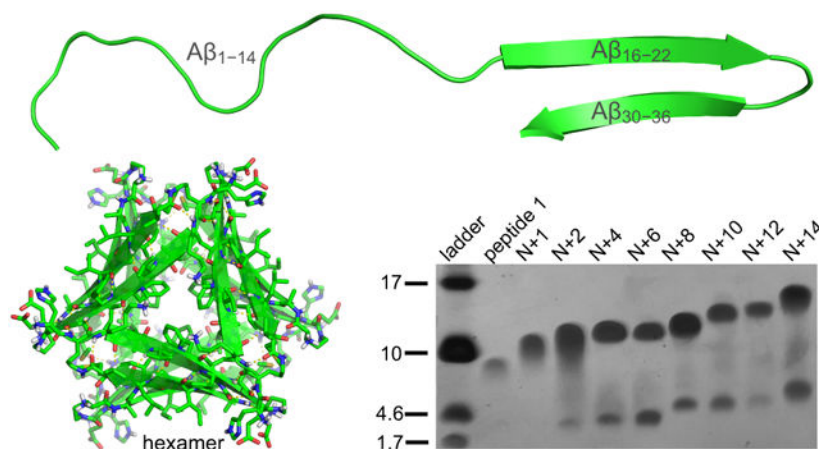
Supporting Information

The Supporting Information is available free of charge on the ACS Publications website at <http://pubs.acs.org/>.

(1) Procedures for the synthesis of peptides **1**, **N+1** through **N+14**, **N+14Me**, SDS-PAGE and silver staining, western blot analysis, circular dichroism studies, LDH-release assays, and size exclusion chromatography; (2) details of X-ray crystallographic data collection, processing, and refinement; (3) characterization data for peptide **N+1** (PDF). Crystallographic data for peptide **N+1** (cif file).

Crystallographic coordinates of peptide **N+1** were deposited into the Protein Data Band (PDB) with code 6VU4.

The authors declare no competing financial interest.



## INTRODUCTION

The first 16 residues of the  $\beta$ -amyloid peptide are thought to be important in the formation of fibrils and oligomers in Alzheimer's disease. These *N*-terminal residues of  $A\beta$  are subject to many important mutations and post-translational modifications, and may interact with other proteins and metal cations.<sup>1-7</sup> These modifications and interactions have been observed to greatly affect  $A\beta$  fibril formation and oligomerization. Even without modification, these residues—<sub>1</sub>DAEFRHDSGYEVHHQK<sub>16</sub>—represent a significant number of amino acids capable of forming non-covalent interactions within and between monomers of  $A\beta$ , and should thus impact oligomerization.

Further supporting the importance of the *N*-terminus of  $A\beta$  are studies of the p3 peptide, an alternative cleavage product to full-length  $A\beta$  from the amyloid precursor protein.<sup>8</sup> The p3 peptide, which lacks residues 1–16 has been described as “nonamyloidogenic”, incapable of forming oligomers, devoid of any synaptotoxic effect, and even neuroprotective<sup>9-13</sup> However, a recent review from the Raskatov group has highlighted and summarized inconsistencies within the literature regarding biophysical and biological properties of the p3 peptide and its importance in Alzheimer's disease.<sup>14-16</sup> In a subsequent investigation, the Raskatov group demonstrated that the p3 peptide is capable of assembling to form amyloidogenic fibrils and toxic oligomers.<sup>17</sup> These recent findings suggest that  $A\beta_{1-16}$  may actually be less important than thought.

Elucidating the role of  $A\beta_{1-16}$  in the formation of  $A\beta$  oligomers offers the promise of furthering our understanding of the molecular basis of Alzheimer's disease. Studying these oligomers is difficult, as these assemblies are heterogeneous—varying in structure, stability, and stoichiometry. Further compounding the challenge of studying  $A\beta$ , is its propensity to form insoluble fibrils, which are more stable than oligomers.  $A\beta$  oligomers are damaging to neurons and are thought to be present in the early stages of Alzheimer's disease before the emergence of any pathohistological hallmarks or dementia symptoms.<sup>18-21</sup>

The assembly of  $A\beta$  oligomers has been tied to the ability of the  $A\beta$  peptide to fold and adopt a  $\beta$ -hairpin conformation.<sup>22,23</sup> In 2008, Hard and Hoyer determined by NMR

spectroscopy that A $\beta$ <sub>1–40</sub> adopts a  $\beta$ -hairpin structure when bound to an affibody. In this structure, residues 17–23 and 30–36 hydrogen bond to form an antiparallel  $\beta$ -sheet, with residues 24–29 as a loop, and the *N*- and *C*-terminal residues as unstructured segments. Our own investigations of peptides derived from the central and *C*-terminal regions of A $\beta$  have revealed that adoption of a  $\beta$ -hairpin conformation primes the peptide to assemble.<sup>24–29</sup>

In 2016, our laboratory reported peptide **1**, a  $\beta$ -hairpin mimic derived from A $\beta$ <sub>16–36</sub> that forms hexamers that can be observed by X-ray crystallography and SDS-PAGE.<sup>28</sup> The peptide is cytotoxic toward SH-SY5Y cells, and cytotoxicity correlates with oligomer formation in structure-activity studies. Peptide **1** contains the heptapeptide fragments A $\beta$ <sub>16–22</sub> and A $\beta$ <sub>30–36</sub> in the “top” and “bottom”  $\beta$ -strands, that are constrained to an antiparallel  $\beta$ -sheet by two turn units of  $\delta$ -linked ornithine,  $\delta$ Orn (Figure 1).<sup>30</sup> The  $\delta$ Orn that links Glu<sub>22</sub> to Ala<sub>30</sub> replaces a loop comprising residues 23–29, while the  $\delta$ Orn that links Lys<sub>16</sub> to Val<sub>36</sub> helps constrain the peptide to a  $\beta$ -hairpin conformation. We incorporate an *N*-methyl group at the center of the top strand, on Phe<sub>19</sub>, to prevent uncontrolled aggregation and fibril formation.

Although peptide **1** has provided insights into the structure, biophysical, and biological properties of hexamers formed by hydrophobic segments of A $\beta$ , it lacks the important *N*-terminal region. In our initial report, REMD simulations of peptide **1** suggested that the hexamer could accommodate *N*- and *C*-terminal extensions without steric clashes.<sup>28</sup> In this investigation, we set out to test experimentally whether the hexamer could accommodate the *N*-terminus and to study the effects of the *N*-terminus on the structure, biophysical, and biological properties of the hexamer. Here we describe the synthesis of *N*-terminally extended homologues of peptide **1**. These *N*-terminally extended homologues bear “tails” of residues derived from A $\beta$ <sub>1–14</sub> and vary in length from 1 to 14 residues. Peptide **N+14**, which contains the entire *N*-terminus, is depicted in Figure 1. Peptides **1**, **N+14**, and other *N*-terminally extended homologues form hexamers in SDS-PAGE, and trimers and dimers in size exclusion chromatography (SEC). Peptide **N+1**, which contains a tail comprising A $\beta$ <sub>14</sub>, forms a hexamer composed of dimers and trimers in the X-ray crystallographic structure. These observations are significant because they may help bridge the gap in our knowledge of how A $\beta$  oligomers assemble in the brain.

## RESULTS AND DISCUSSION

### Synthesis of Peptide **N+14**.

We synthesized peptide **N+14** by Fmoc-based solid phase peptide synthesis, using Fmoc-Orn(Dde)-OH to incorporate an *N*-terminal tail of residues derived from A $\beta$ <sub>1–14</sub> (Figure 2). We began the synthesis by attaching Boc-Orn(Fmoc)-OH to 2-chlorotrityl resin. Residues 22 through 2 were then introduced by Fmoc-based SPPS using HCTU as the coupling reagent, with Fmoc-Orn(Dde)-OH replacing residue 15 in the natural sequence of A $\beta$ . Residue 1 was coupled as Boc-Asp(*t*-Bu)-OH, capping the synthesis of the top strand. The Dde protecting group was then removed with 10% hydrazine in DMF, and residues 36 through 30 were coupled to residue 15 using Fmoc-based SPPS. We found microwave-assisted SPPS to be essential and used it for most of the coupling steps, other than attaching Boc-Orn(Fmoc)-OH to the resin and removing the Dde protecting group.<sup>31</sup> The final Fmoc protecting group was

removed from residue 30, and the acyclic branched peptide was cleaved from the resin with a solution of 20% HFIP in DCM. The peptide was cyclized with PyBop in solution, and deprotected with treatment by trifluoroacetic acid (TFA). Purification by reverse-phase HPLC typically afforded ca. 12 mg peptide **N+14** as the trifluoroacetate salt.<sup>32,33</sup>

### Oligomerization and Folding of Peptides **1** and **N+14**.

We studied the assembly and folding of peptide **1** and peptide **N+14** by SDS-PAGE, western blot, circular dichroism (CD) spectroscopy, and a cytotoxicity assay with SH-SY5Y cells. Like the A $\beta$  peptide, peptide **1** and peptide **N+14** assemble to form oligomers in SDS-PAGE. We have previously reported peptide **1** (1.77 kDa) to run in SDS-PAGE with a molecular weight consistent with that of a hexamer (Figure 3A).<sup>28</sup> The band formed by peptide **1** is comet shaped and streaks downward from the 10 kDa ladder band, suggesting that the hexamer may be in rapid equilibrium with lower molecular weight species. An X-ray crystallographic structure of peptide **1** (PDB 5W4H) further corroborates the formation of a hexamer. In contrast to peptide **1**, the *N*-terminally extended homologue peptide **N+14** (3.45 kDa) forms two species by SDS-PAGE, which appear to be in slow equilibrium. One is an oligomer that migrates to just below the 17 kDa ladder band, which we interpret as a hexamer. The other migrates just above the 4.6 kDa ladder band, which we interpret as a dimer. The hexamer band formed by peptide **N+14** in silver-stained SDS-PAGE is more intense than the putative dimer band, suggesting that this oligomer predominates at the 75  $\mu$ M concentration under which the gel was run. These SDS-PAGE studies show that the hexamer can accommodate residues 1–14, but that introduction of these residues appears to substantially reduce the rate of exchange between the hexamer and lower order species.

To compare the oligomerization of peptide **N+14** to full-length A $\beta$ , we performed SDS-PAGE in a western blot against A $\beta$ <sub>M1–42</sub>, using the 6E10 antibody to visualize the bands generated by each peptide (Figure S1).<sup>34–36</sup> The 6E10 antibody recognizes the *N*-terminal epitope comprising residues Arg<sub>5</sub>-His<sub>6</sub>-Asp<sub>7</sub>, which is shared by both peptide **N+14** and full-length A $\beta$ .<sup>37</sup> A $\beta$ <sub>M1–42</sub> shows a strong band for the monomer, as well as weaker bands for oligomers. In contrast, the hexamer band for peptide **N+14** predominates. This difference in oligomerization may reflect the lack of stabilizing conformational constraints in the A $\beta$ <sub>M1–42</sub> peptide.<sup>23</sup> In peptide **N+14**, the  $\delta$ Orn turn units help prime the peptide for assembly by stabilizing a  $\beta$ -hairpin conformation.

In the hexamer formed by peptide **1**, the bottom edges of the monomer subunits hydrogen bond to each other. To test whether peptide **N+14** assembles to form a similar hexamer, we prepared and studied peptide **N+14**<sub>Me</sub>, a homologue of peptide **N+14** with an additional *N*-methyl group on Gly<sub>33</sub> (Figure 4). In the hexamer formed by peptide **1**, this additional *N*-methyl group has been shown to disrupt hydrogen bonding between Gly<sub>33</sub> of one monomer and Ile<sub>31</sub> of the adjacent monomer within the dimer subunit, thus interfering with assembly (Figure S2).<sup>28,38</sup> If peptide **N+14** assembles to form a hexamer similar to peptide **1**, *N*-methylation of Gly<sub>33</sub> should also disrupt assembly of the hexamer. By SDS-PAGE, peptide **N+14**<sub>Me</sub> migrates as a single band that runs parallel to the putative dimer band formed by peptide **N+14** (Figure 3A). In contrast to peptide **N+14**, peptide **N+14**<sub>Me</sub> does not form a hexamer band. The migration of peptide **N+14**<sub>Me</sub> confirms that *N*-methylation of Gly<sub>33</sub> in

peptide **N+14** disrupts the assembly of higher order oligomers, and provides further evidence that peptide **N+14** assembles to form a hexamer similar in structure to peptide **1**.

Peptide **1** adopts a  $\beta$ -hairpin conformation in the crystallographic hexamer.<sup>28</sup> In aqueous solution—where size exclusion chromatography (SEC) studies have shown peptide **1** to exist as a mixture of monomer, dimer, and trimer—circular dichroism (CD) studies suggest that peptide **1** also adopts a  $\beta$ -hairpin conformation (Figure 3B).<sup>28</sup> The CD spectrum of peptide **1** displays a negative band centered at ca. 210 nm, with increasing ellipticity at lower wavelengths and a positive ellipticity below 192 nm. To evaluate the ability of peptide **N+14** to adopt a  $\beta$ -hairpin, we compared the CD spectrum of peptide **N+14** to that of peptide **1** (Figure 3B). The CD spectrum of peptide **N+14** is substantially shallower than the CD spectrum of peptide **1**, with a weaker negative band centered at a slightly lower wavelength and no positive ellipticity above 190 nm. This spectrum appears to reflect an ensemble of  $\beta$ -hairpin and random coil conformations. The CD spectrum of peptide **N+14<sub>Me</sub>** is similar to that of peptide **N+14**, suggesting that the additional *N*-methyl group on Gly<sub>33</sub> does not substantially alter the folding of peptide **N+14<sub>Me</sub>**.

To better understand the CD spectrum of peptide **N+14**—in particular how residues 1–14 affect the  $\beta$ -hairpin formed by residues 16–22 and 30–36—we synthesized peptide **2**, the *C*-terminal amide of A $\beta$ <sub>1-14</sub> (H-DAEFRHDSGYEVHH-NH<sub>2</sub>). The CD spectrum of peptide **2** shows a strong negative band at ca. 190 nm and a weak positive band centered at ca. 220 nm, reflecting a predominantly random coil conformation (Figure 3C). To test whether the spectrum of peptide **N+14** represents a linear combination of peptide **1** and peptide **2**, we combined both peptides in equimolar concentrations and acquired the CD spectrum of the mixture. The CD spectrum of the mixture shows a negative band centered at ca. 208 nm with no positive band above 190 nm. Like the CD spectrum of peptide **N+14**, the spectrum of the mixture shows a diminished  $\beta$ -sheet-like conformation relative to peptide **1**.

To evaluate the cytotoxicity of peptide **N+14**, we compared it to peptide **1** in an LDH release assay against neuronally derived SH-SY5Y cells. We had previously reported that peptide **1** was toxic at concentrations of 50  $\mu$ M or higher.<sup>28</sup> Peptide **N+14** proved less cytotoxic than peptide **1**, even though it contains more residues from the sequence of full-length A $\beta$  (Figure S3). The addition of residues 1–14 to peptide **1** does not enhance cytotoxicity, but rather diminishes the cytotoxicity. We envision that the cytotoxicity of peptide **1** is predominantly driven by the hydrophobic residues from the central region of A $\beta$ , 16–22 and 30–36, and their interactions with cell membranes. These hydrophobic membrane interactions are likely offset by the hydrophilic tail in peptide **N+14**.

### Oligomerization and Folding of Shorter *N*-Terminally Extended Homologues.

To gain additional insights into the effects of *N*-terminal extension on the assembly of peptide **1**, we prepared seven additional *N*-terminally extended homologues of peptide **N+14** with shorter *N*-terminal tails: peptides **N+1**, **N+2**, **N+4**, **N+6**, **N+8**, **N+10**, and **N+12** (Figure 5). The CD spectra of these peptides all show minima between 210 and 220 nm (Figure 6). The minima are generally deeper for the peptides bearing shorter *N*-terminal extensions (**N+1** through **N+4**) (Figure 6A), and shallower for the peptides bearing longer *N*-terminal

extensions (**N+6** through **N+12**) (Figure 6B). These differences reflect increased random coil character of the larger *N*-terminal extensions. The depth of the minimum of peptide **N+1** ( $\Theta = -6190 \text{ deg cm}^2 \text{ dmol}^{-1}$ ) is substantially less than that of peptide **1** ( $\Theta = -9516 \text{ deg cm}^2 \text{ dmol}^{-1}$ ). This difference cannot be explained by a random coil conformation of the additional single residue, but rather suggests that *N*-acylation of the  $\delta$ -linked ornithine turn unit diminishes the  $\beta$ -sheet folding of the macrocycle.<sup>39,40</sup>

To determine the impact of these *N*-terminal extensions on the oligomerization of peptide **1**, we compared the assembly of peptide **1** and each *N*-terminally extended peptide using SDS-PAGE (Figure 7). We included trimers **1** and **2** as molecular-weight standards for comparison (Figures S4 and S5). Trimer **1** (5.3 kDa) and trimer **2** (5.3 kDa) are covalently stabilized trimers of  $\beta$ -hairpin peptides that we have previously reported to self-assemble and migrate respectively as 10.6 kDa hexamers and 21.2 kDa dodecamers.<sup>26</sup> SDS-PAGE reveals that each *N*-terminally extended peptide migrates as a hexamer. Peptide **1** migrates to approximately the same position as trimer **1**, and each of the longer *N*-terminally extended peptides migrates at a position between the hexamer formed by trimer **1** and the dodecamer formed by trimer **2**. The hexamer formed by peptide **N+1** (1.91 kDa) migrates to the top of the 10 kDa ladder band and streaks downward like peptide **1**. Similarly, the hexamer formed by peptide **N+2** (2.05 kDa) migrates to just above the 10 kDa ladder band and also streaks downward. The streaking observed for peptides **N+1** and **N+2** suggests that the hexamers formed by each peptide are in equilibrium with smaller oligomers. The hexamer bands formed by peptides **N+4** (2.28 kDa), **N+6** (2.49 kDa), **N+8** (2.69 kDa), **N+10** (2.99 kDa), **N+12** (3.27 kDa), and **N+14** (3.45 kDa) are in comparable or higher positions than peptide **N+2** and migrate as tight bands between the 10 and 17 kDa ladder bands. The tightness of these bands may reflect an increase in hexamer stability that arises from stabilizing non-covalent interactions from the *N*-terminal tail. Peptides **N+2** through **N+14** also show bands at or above the 4.6 kDa ladder band which correspond to the putative dimer.

To quantitatively assess the relationship between oligomer assembly and migration, we plotted the logarithm of oligomer molecular weights against the relative migration distance ( $R_f$ ) of the hexamer bands (Figure 8). The ladder bands exhibit an excellent correlation between  $\log \text{ MW}$  and  $R_f$  ( $R^2 = 0.999$ , black), with the exception of the 1.7 kDa ladder band which was excluded from the analysis. The hexamers do not fall on this line, but rather are shifted 12–33% lower than their calculated molecular weights, thus appearing as pentamers or tetramers. The hexamer bands also exhibit a linear relationship between  $\log \text{ MW}$  and  $R_f$ , albeit with a poorer fit to a straight line ( $R^2 = 0.881$ , red). For comparison we also plotted the  $\log \text{ MW}$  vs.  $R_f$  for the covalently stabilized trimers **1** and **2** (green), which run on the gel as hexamers and dodecamers. These oligomers fall slightly off the line for the ladder bands.

Membrane proteins often migrate by SDS-PAGE at an apparent molecular weight that does not correspond to the actual molecular weight of the protein.<sup>41-43</sup> Often this “gel shifting” results in a lower apparent molecular weight. This behavior has been well characterized for full-length A $\beta$  and linear truncated variants of A $\beta$ , where SDS binding correlates with hydrophobicity rather than the number of amino acids.<sup>44</sup> The low apparent molecular weights of the hexamer bands may thus reflect gel shifting, causing the hexamer bands to appear as smaller oligomers (pentamers or tetramers).

We used size exclusion chromatography (SEC) to better understand the solution-phase assembly of these *N*-terminally extended peptides. In SEC, peptide **1** does not assemble to form a hexamer (Figure 9). Peptide **1** elutes as a broad band comprising a large peak at 20.2 mL, a smaller peak at 19.1 mL, and a small peak at 17.9 mL.<sup>28</sup> These elution volumes fall at the low molecular weight range of the column, near the size standards vitamin B12 (1.3 kDa, 19.7 mL) and aprotinin (6.5 kDa, 16.8 mL). Thus, the three peaks from peptide **1** appear to correspond to a monomer, a dimer, and a trimer (1.8 kDa, 3.6 kDa, and 5.3 kDa). Peptides **N+1** through **N+14** also run as broad bands that contain multiple features (Figure 9). The SEC traces of the *N*-terminally extended homologues exhibit main bands between peptide **1** and the aprotinin size standard and additional minor peaks that elute significantly after peptide **1**. The main bands are composed of several peaks which appear to correspond to monomer, dimer, and trimer. The *N*-terminally extended peptides also exhibit additional peaks that elute after vitamin B12, which may reflect adsorption of the peptides to the column.

The broad band formed by peptide **N+14** shows a different distribution of monomer, dimer, and trimer peaks than peptide **1**. Peptide **N+14** elutes with a large peak at 17.4 mL, a smaller peak at 18.7 mL, and a small shoulder at 20.1 mL (Figure 9). We interpret these peaks to be the trimer (10.5 kDa), dimer (6.5 kDa), and monomer (3.5 kDa) of peptide **N+14**. The SEC trace of peptide **N+12** resembles the SEC trace of peptide **N+14** (Figure S6). The SEC traces of peptides **N+1**, **N+2**, and **N+4** resemble the SEC trace of peptide **1** (Figure S7). The SEC traces of peptides **N+6**, **N+8**, and **N+10** differ from the SEC traces of peptide **1** and peptide **N+14** (Figure S8). The SEC traces of peptides **N+6**, **N+8**, and **N+10** show two peaks, which correspond to a monomer peak and a dimer or trimer peak.

As controls we performed SEC on peptide **2** ( $A\beta_{1-14}$ , H-DAEFRHDSGYEVHH-NH<sub>2</sub>) and peptide **N+14<sub>Me</sub>**. Peptides **2** and **N+14<sub>Me</sub>** elute between the vitamin B12 and aprotinin size standards (Figure S9). Peptide **2** elutes as a narrow band at 17.6 mL that corresponds to a monomer. Peptide **N+14<sub>Me</sub>** elutes as a broader band at 18.9 mL that may correspond to monomer and/or dimer. Elution volumes for each peptide are summarized in supplementary Table 2.

To better assess the relationship between the assembly and elution volumes amongst the *N*-terminally extended homologues, we plotted the logarithm of the oligomer molecular weight against the elution volumes for peptide **1** and peptides **N+1** through **N+14** (Figure 10). The resulting graph revealed a linear relationship between the monomer, dimer, and trimer elution volumes, with increasing oligomer size correlating with decreased elution volumes. Collectively, the SEC studies show that at hundred micromolar concentrations, peptide **1** and peptides **N+1** through **N+14** form mixtures of monomers, dimers, and trimers that equilibrate slowly on the 40-minute time scale of the SEC experiment.<sup>45</sup>

The SDS-PAGE and SEC studies reveal that *N*-terminally extended homologues of peptide **1** can assemble to form oligomers in aqueous environments in the presence or absence of sodium dodecyl sulfate. In SDS-PAGE, peptide **1** and each of the *N*-terminally extended homologues form hexamers. In SEC, peptide **1** and each of the *N*-terminally extended homologues do not form hexamers, but rather appear to elute as monomers, dimers, and

trimers. The lipophilic environment produced by the SDS micelles in SDS-PAGE appears to drive the assembly of the hexamers.<sup>46-48</sup>

### X-ray crystallographic structure of peptide N+1.

X-ray crystallography of peptide N+1 (PDB 6VU4) corroborates the formation of the hexamers observed in SDS-PAGE (Figures 11 and 12). Peptide N+1 afforded crystals suitable for X-ray diffraction from an aqueous solution containing 0.1 M HEPES buffer at pH 7.2, 0.2 M sodium citrate, and 25% isopropanol. X-ray diffraction data were collected at a resolution of 2.08 Å. The crystallographic phase determination was carried out through molecular replacement using the structure of peptide 1 (PDB 5W4H) as the search model. Supplementary Table 3 summarizes the crystallographic properties, crystallization conditions, data collection, and model refinement statistics for peptide N+1.

In the crystal structure, the asymmetric unit contains two molecules of peptide N+1 that assemble edge-to-edge to form an out-of-register, antiparallel  $\beta$ -sheet dimer. Each monomer subunit folds to form a twisted  $\beta$ -hairpin stabilized by eight intramolecular hydrogen bonds between the top and bottom  $\beta$ -strands. The dimer itself is stabilized by four intermolecular hydrogen bonds between Ile<sub>31</sub> and Gly<sub>33</sub> in the bottom strands of both macrocycles (Figures 11A and S10). Three dimers further assemble to form a hexamer—a trimer of dimers—that is nearly identical to the hexamer formed by peptide 1 (Figure S11). The hexamer can also be interpreted as a dimer of trimers formed through face-to-face packing of two trimers (Figure 11B and S10). Each vertex of the trimer is stabilized by three hydrogen bonds: two between Ala<sub>21</sub> and  $\delta$ Orn, and one between *N*-Me-Phe<sub>19</sub> and Leu<sub>17</sub> (a total of nine hydrogen bonds per trimer). The hexamer is further stabilized by the packing of six sets of hydrophobic side chains from Leu<sub>17</sub>, *N*-Me-Phe<sub>19</sub>, Ala<sub>21</sub>, Ile<sub>31</sub>, and Met<sub>35</sub> (Figure S10). In each of the two crystallographically independent monomers of peptide N+1, His<sub>14</sub> is clearly visible in the electron density map, further corroborating that the hexamer can accommodate the *N*-terminal A $\beta$  residues (Figure 11C).

## SUMMARY AND CONCLUSION

To better mimic oligomers of full length A $\beta$ , we have appended residues from A $\beta$ <sub>1-14</sub> as an *N*-terminal tail to macrocyclic  $\beta$ -hairpin peptide 1, which comprises A $\beta$ <sub>16-22</sub> and A $\beta$ <sub>30-36</sub>. The synthesis of these tailed macrocycles was achieved through an orthogonal protecting group strategy using the amino acid protecting group Dde, in addition to Fmoc and Boc. Circular dichroism revealed that peptide 1 and the *N*-terminally extended homologues adopt  $\beta$ -sheet-like conformations, consistent with a model in which  $\beta$ -hairpins are key components of A $\beta$  oligomers. In aqueous solution, peptide 1 and the *N*-terminally extended homologues form dimers and trimers in SEC, and hexamers in SDS-PAGE. The observations of dimers, trimers, and hexamers in solution are recapitulated in the X-ray crystallographic structure of peptide N+1. The consistent formation of hexamers by peptide 1 and the *N*-terminally extended homologues suggests that the *N*-terminus of A $\beta$  does not substantially modify or impede the assembly of oligomers derived from A $\beta$ <sub>1-36</sub>. These findings are surprising in light of the purported importance of the *N*-terminus in the aggregation of A $\beta$  in Alzheimer's

disease, as they support a model in which the *N*-terminus is not critical for the assembly of A $\beta$  oligomers.<sup>17</sup>

## Supplementary Material

Refer to Web version on PubMed Central for supplementary material.

## ACKNOWLEDGMENTS

We thank the National Institutes of Health (NIH) National Institute of General Medical Sciences (NIGMS) for funding (GM097562). We also thank Dr. Dmitry Fishman and the Laser Spectroscopy Laboratories in the UCI Department of Chemistry for assistance with circular dichroism measurements. M.W. acknowledges the support from the Ministry of Science and Higher Education, Republic of Poland (Mobility Plus grant no. 1647/MOB/V/2017/0).

## REFERENCES AND NOTES

- (1). Murray B; Sharma B; Belfort G *N*-Terminal Hypothesis for Alzheimer's Disease. *ACS Chem. Neurosci* 2017, 8 (3), 432–434. 10.1021/acschemneuro.7b00037. [PubMed: 28186729]
- (2). Kepp KP *Bioinorganic Chemistry of Alzheimer's Disease*. *Chem. Rev* 2012, 112 (10), 5193–5239. 10.1021/cr300009x. [PubMed: 22793492]
- (3). Przygo ska K; Pacewicz M; Sadowska W; Pozna ski J; Bal W; Dadlez M His6, His13, and His14 Residues in A $\beta$ 1 – 40 Peptide Significantly and Specifically Affect Oligomeric Equilibria. *Sci. Rep* 2019, 9, 9449. 10.1038/s41598-019-45988-1. [PubMed: 31263161]
- (4). Przygo ska K; Pozna ski J; Mistrz UH; Rand KD; Dadlez M Side-Chain Moieties from the *N*-Terminal Region of A $\beta$  Are Involved in an Oligomer-Stabilizing Network of Interactions. *PLoS One* 2018, 13 (8), 1–25. 10.1371/journal.pone.0201761.
- (5). Sofola-Adesakin O; Khericha M; Snoeren I; Tsuda L; Partridge L PGLuA $\beta$  Increases Accumulation of A $\beta$  in Vivo and Exacerbates Its Toxicity. *Acta Neuropathol. Commun* 2016, 4 (1), 109. 10.1186/s40478-016-0380-x. [PubMed: 27717375]
- (6). Jawhar S; Wirhth O; Bayer TA Pyroglutamate Amyloid- $\beta$  (A $\beta$ ): A Hatchet Man in Alzheimer Disease. *J. Biol. Chem* 2011, 286 (45), 38825–38832. 10.1074/jbc.R111.288308. [PubMed: 21965666]
- (7). Kummer MP; Heneka MT Truncated and Modified Amyloid-Beta Species. *Alzheimer's Res. Ther* 2014, 6 (3), 1–9. 10.1186/alzrt258. [PubMed: 24382028]
- (8). Moghekar A; Rao S; Li M; Ruben D; Mammen A; Tang X; Brien RJO Large Quantities of A $\beta$  Peptide Are Constitutively Released during Amyloid Precursor Protein Metabolism in Vivo and in Vitro. 2011, 286 (18), 15989–15997. 10.1074/jbc.M110.191262.
- (9). Walsh DM; Klyubin I; Fadeeva JV; Cullen WK; Anwyl R; Wolfe MS; Rowan MJ; Selkoe DJ Naturally Secreted Oligomers of Amyloid Beta Protein Potently Inhibit Hippocampal Long-Term Potentiation in Vivo. *Nature* 2002, 416 (6880), 535–539. [PubMed: 11932745]
- (10). Dulin F; Léveillé F; Ortega JB; Mornon JP; Buisson A; Callebaut I; Colloc'h N P3 Peptide, a Truncated Form of A $\beta$  Devoid of Synaptotoxic Effect, Does Not Assemble into Soluble Oligomers. *FEBS Lett.* 2008, 582 (13), 1865–1870. 10.1016/j.febslet.2008.05.002. [PubMed: 18474239]
- (11). Näslund J; Jensen M; Tjernberg LO; Thyberg J; Terenius L; Nordstedt C The Metabolic Pathway Generating P3, an A $\beta$ -Peptide Fragment, Is Probably NonAmyloidogenic. *Biochemical and Biophysical Research Communications*. 1994, pp 780–787. 10.1006/bbrc.1994.2527.
- (12). Nhan HS; Chiang K; Koo EH The Multifaceted Nature of Amyloid Precursor Protein and Its Proteolytic Fragments: Friends and Foes. *Acta Neuropathol.* 2015, 129 (1), 1–19. 10.1007/s00401-014-1347-2. [PubMed: 25287911]
- (13). Han W; Ji T; Mei B; Su J Peptide P3 May Play a Neuroprotective Role in the Brain. *Med. Hypotheses* 2011, 76 (4), 543–546. 10.1016/j.mehy.2010.12.013. [PubMed: 21255941]

- (14). Kuhn AJ; Raskatov J Is the P3 (AB17-40, AB17-42) Peptide Relevant to the Pathology of Alzheimer's Disease? *J. Alzheimer's Dis* 2020, 74 (1), 43–53. [PubMed: 32176648]
- (15). Pike CJ; Overman MJ; Cotman CW Amino-Terminal Deletions Enhance Aggregation of  $\beta$ -Amyloid Peptides in Vitro. *J. Biol. Chem* 1995, 23895–23898. [PubMed: 7592576]
- (16). Lalowski M; Golabek A; Lemere CA; Selkoe DJ; Wisniewski HM; Beavis RC; Frangione B; Wisniewski T The “Nonamyloidogenic” P3 Fragment (Amyloid B17-42) Is a Major Constituent of Down's Syndrome Cerebellar Preamyloid. *J. Biol. Chem* 1996, 271 (52), 33623–33631. 10.1074/jbc.271.52.33623. [PubMed: 8969231]
- (17). Kuhn AJ; Abrams BS; Knowlton S; Raskatov JA The Alzheimer's Disease “Non-Amyloidogenic” P3 Peptide Revisited: A Case for Amyloid- $\alpha$ . *ACS Chem. Neurosci* 2020, 11, 11, 1539–1544. 10.1021/acscemneuro.0c00160. [PubMed: 32412731]
- (18). Cline EN; Bicca MA; Viola KL; Klein WL The Amyloid- $\beta$  Oligomer Hypothesis: Beginning of the Third Decade. *J. Alzheimer's Dis* 2018, 64 (s1), S567–S610. 10.3233/JAD-179941. [PubMed: 29843241]
- (19). Ferreira ST; Lourenco MV; Oliveira MM; De Felice FG Soluble Amyloid-B Oligomers as Synaptotoxins Leading to Cognitive Impairment in Alzheimer's Disease. *Front. Cell. Neurosci* 2015, 9, 1–17. 10.3389/fncel.2015.00191. [PubMed: 25667569]
- (20). Benilova I; Karran E; De Strooper B The Toxic A $\beta$  Oligomer and Alzheimer's Disease: An Emperor in Need of Clothes. *Nat. Neurosci* 2012, 15 (3), 349–357. 10.1038/nn.3028. [PubMed: 22286176]
- (21). Selkoe DJ; Hardy J The Amyloid Hypothesis of Alzheimer's Disease at 25 Years. *EMBO Mol. Med* 2016, 8 (6), 595–608. 10.15252/emmm.201606210. [PubMed: 27025652]
- (22). Hoyer W; Gronwall C; Jonsson A; Stahl S; Hard T Stabilization of a  $\beta$ -Hairpin in Monomeric Alzheimer's Amyloid- $\beta$  Peptide Inhibits Amyloid Formation. *Proc. Natl. Acad. Sci* 2008, 105 (13), 5099–5104. 10.1073/pnas.0711731105. [PubMed: 18375754]
- (23). Sandberg A; Luheshi LM; Sollvander S; Pereira de Barros T; Macao B; Knowles TPJ; Biverstal H; Lendel C; Ekholm-Pettersson F; Dubnovitsky A; Lannfelt L; Dobson CM; Hard T Stabilization of Neurotoxic Alzheimer Amyloid- $\beta$  Oligomers by Protein Engineering. *Proc. Natl. Acad. Sci. U.S.A* 2010, 107 (35), 15595–15600. 10.1073/pnas.1001740107. [PubMed: 20713699]
- (24). Spencer RK; Li H; Nowick JS X-Ray Crystallographic Structures of Trimers and Higher-Order Oligomeric Assemblies of a Peptide Derived from A $\beta$ 17-36. *J. Am. Chem. Soc* 2014, 136 (15), 5595–5598. 10.1021/ja5017409. [PubMed: 24669800]
- (25). Kreutzer AG; Hamza IL; Spencer RK; Nowick JS X-Ray Crystallographic Structures of a Trimer, Dodecamer, and Annular Pore Formed by an A $\beta$ 17-36  $\beta$ -Hairpin. *J. Am. Chem. Soc* 2016, 138 (13), 4634–4642. 10.1021/jacs.6b01332. [PubMed: 26967810]
- (26). Kreutzer AG; Yoo S; Spencer RK; Nowick JS Stabilization, Assembly, and Toxicity of Trimers Derived from A $\beta$ . *J. Am. Chem. Soc* 2017, 139 (2), 966–975. 10.1021/jacs.6b11748. [PubMed: 28001392]
- (27). Salveson PJ; Spencer RK; Kreutzer AG; Nowick JS X-Ray Crystallographic Structure of a Compact Dodecamer from a Peptide Derived from A $\beta$  16–36. *Org. Lett* 2017, 19, 3465. 10.1021/acscorglett.7b01445.
- (28). Kreutzer AG; Spencer RK; McKnelly KJ; Yoo S; Hamza IL; Salveson PJ; Nowick JS A Hexamer of a Peptide Derived from A $\beta$ 16-36. *Biochemistry* 2017, 56 (45), 6061–6071. 10.1021/acsbiochem.7b00831. [PubMed: 29028351]
- (29). Kreutzer AG; Nowick JS Elucidating the Structures of Amyloid Oligomers with Macrocyclic  $\beta$ -Hairpin Peptides: Insights into Alzheimer's Disease and Other Amyloid Diseases. *Acc. Chem. Res* 2018, 51 (3), 706–718. 10.1021/acs.accounts.7b00554. [PubMed: 29508987]
- (30). Nowick JS; Brower JO A New Turn Structure for the Formation of  $\beta$ -Hairpins in Peptides. *J. Am. Chem. Soc* 2003, 125 (4), 876–877. 10.1021/ja028938a. [PubMed: 12537479]
- (31). Attempts to synthesize peptide **N+14** by manual coupling at room temperature resulted in poor resin swelling and complex mixtures of products containing only traces of peptide **N+14**.
- (32). The use of uronium coupling agents during macrolactamization results in the formation of a tetramethylguanidylated adduct as an impurity that is difficult to separate from the desired peptide. The use of the phosphonium coupling agent PyBOP circumvents this problem.

- (33). Albericio F; Bofill JM; El-Faham A; Kates SA Use of Onium Salt-Based Coupling Reagents in Peptide Synthesis. *J. Org. Chem* 1998, 63 (26), 9678–9683. 10.1021/jo980807y.
- (34). A $\beta$ <sub>M1-42</sub> is an expressed homologue of A $\beta$ <sub>1-42</sub> that bears an additional methionine at the *N*-terminus and exhibits similar aggregation properties to A $\beta$ <sub>1-42</sub>.
- (35). Yoo S; Zhang S; Kreutzer AG; Nowick JS An Efficient Method for the Expression and Purification of A $\beta$ (M1-42). *Biochemistry* 2018, 57 (26), 3861–3866. 10.1021/acs.biochem.8b00393. [PubMed: 29757632]
- (36). Walsh DM; Thulin E; Minogue AM; Gustavsson N; Pang E; Teplow DB; Linse S A Facile Method for Expression and Purification of the Alzheimer's Disease-Associated Amyloid  $\beta$ -Peptide. *FEBS J.* 2009, 276 (5), 1266–1281. 10.1111/j.1742-4658.2008.06862.x. [PubMed: 19175671]
- (37). Baghallab I; Reyes-Ruiz JM; Abulnaja K; Huwait E; Glabe C Epitomic Characterization of the Specificity of the Anti-Amyloid A $\beta$  Monoclonal Antibodies 6E10 and 4G8. *J. Alzheimer's Dis* 2018, 66 (3), 1235–1244. 10.3233/JAD-180582. [PubMed: 30412489]
- (38). Salvesson PJ; Haerianardakani S; Thuy-Boun A; Kreutzer AG; Nowick JS Controlling the Oligomerization State of A $\beta$ -Derived Peptides with Light. *J. Am. Chem. Soc* 2018, 140 (17), 5842–5852. 10.1021/jacs.8b02658. [PubMed: 29627987]
- (39). Woods RJ; Brower JO; Castellanos E; Hashemzadeh M; Khakshoor O; Russu WA; Nowick JS Cyclic Modular  $\beta$ -Sheets. *J. Am. Chem. Soc* 2007, 129 (9), 2548–2558. 10.1021/ja0667965. [PubMed: 17295482]
- (40). The minima of the *N*-terminally extended homologues are substantially shallower than that of peptide **1**. Out of concern that the weaker minima might reflect substantial differences in concentration across the samples, we measured the absorbance of each peptide at 214 nm (A<sub>214</sub>) and normalized for number of residues (n). The A<sub>214</sub>/n values of each peptide (peptides **N+1** through **N+14**) were all within  $\pm$  17% of the A<sub>214</sub>/n value of peptide **1**. These data are summarized in Table S1 in the Supporting Information.
- (41). Rath A; Glibowicka M; Nadeau VG; Chen G; Deber CM Detergent Binding Explains Anomalous SDS-PAGE Migration of Membrane Proteins. 2009, 106 (6), 1760–1765.
- (42). Tulumello DV; Deber CM SDS Micelles as a Membrane-Mimetic Environment for Transmembrane Segments. *Biochemistry* 2009, 48, 51, 12096–12103. 10.1021/bi9013819. [PubMed: 19921933]
- (43). Shi Y; Mowery RA; Ashley J; Hentz M; Ramirez AJ; Bilgicer B; Slunt-brown H; Borchelt DR; Shaw BF Abnormal SDS-PAGE Migration of Cytosolic Proteins Can Identify Domains and Mechanisms That Control Surfactant Binding. *Protein Science* 2012, 21, 5–7. 10.1002/pro.2107.
- (44). Kawooya JK; Emmons TL; Gonzalez-dewhitt PA; Camp MC; Andrea SCD Electrophoretic Mobility of Alzheimers Amyloid- $\beta$  Peptides in Urea – Sodium Dodecyl Sulfate – Polyacrylamide Gel Electrophoresis. *Analytical Biochemistry* 2003, 323, 103–113. 10.1016/j.ab.2003.08.027. [PubMed: 14622964]
- (45). Solutions of peptide **1** and peptides **N+1** through **N+14** were prepared at 1.0 mg/mL (0.2 – 0.5 mM) in Tris buffer. Insoluble material was removed by centrifugation prior to injection onto the SEC column. The actual concentrations after centrifugation were estimated to be between 50 and 100  $\mu$ M on the basis of absorbance at 214 nm (Supplementary Table 2).
- (46). Nowick JS; Chen JS Molecular Recognition in Aqueous Micellar Solution: Adenine-Thymine Base-Pairing in SDS Micelles. *J. Am. Chem. Soc* 1992, 114 (3), 1107–1108. 10.1021/ja00029a060.
- (47). Nowick JS; Chen JS; Noronha G Molecular Recognition in Micelles: The Roles of Hydrogen Bonding and Hydrophobicity in Adenine-Thymine Base-Pairing in SDS Micelles. *J. Am. Chem. Soc* 1993, 115 (17), 7636–7644. 10.1021/ja00070a007.
- (48). Nowick JS; Cao T; Noronha G Molecular Recognition between Uncharged Molecules in Aqueous Micelles. *J. Am. Chem. Soc* 1994, 116 (8), 3285–3289. 10.1021/ja00087a014. [PubMed: 25084234]

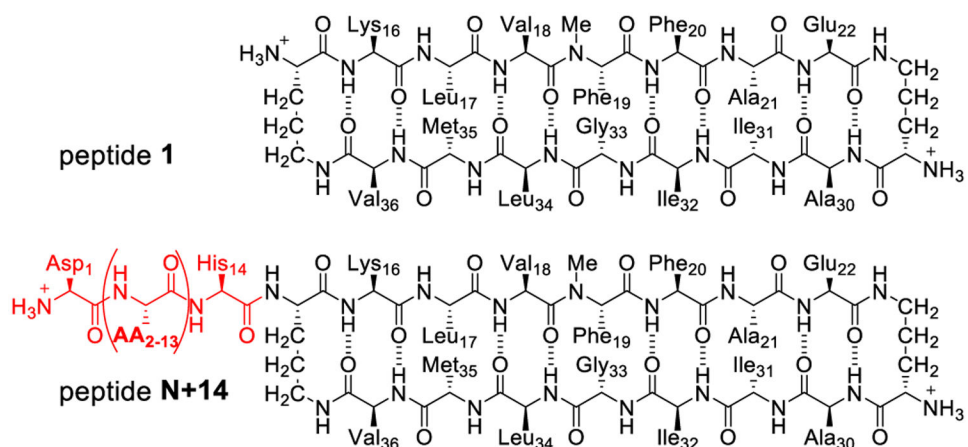


**Figure 1.**

Extending the *N*-terminus of peptide **1** to include residues 1–14 as an *N*-terminal tail (red), giving peptide **N+14**. Residues in the tail comprise Asp<sub>1</sub>, Ala<sub>2</sub>, Glu<sub>3</sub>, Phe<sub>4</sub>, Arg<sub>5</sub>, His<sub>6</sub>, Asp<sub>7</sub>, Ser<sub>8</sub>, Gly<sub>9</sub>, Tyr<sub>10</sub>, Glu<sub>11</sub>, Val<sub>12</sub>, His<sub>13</sub>, and His<sub>14</sub>.

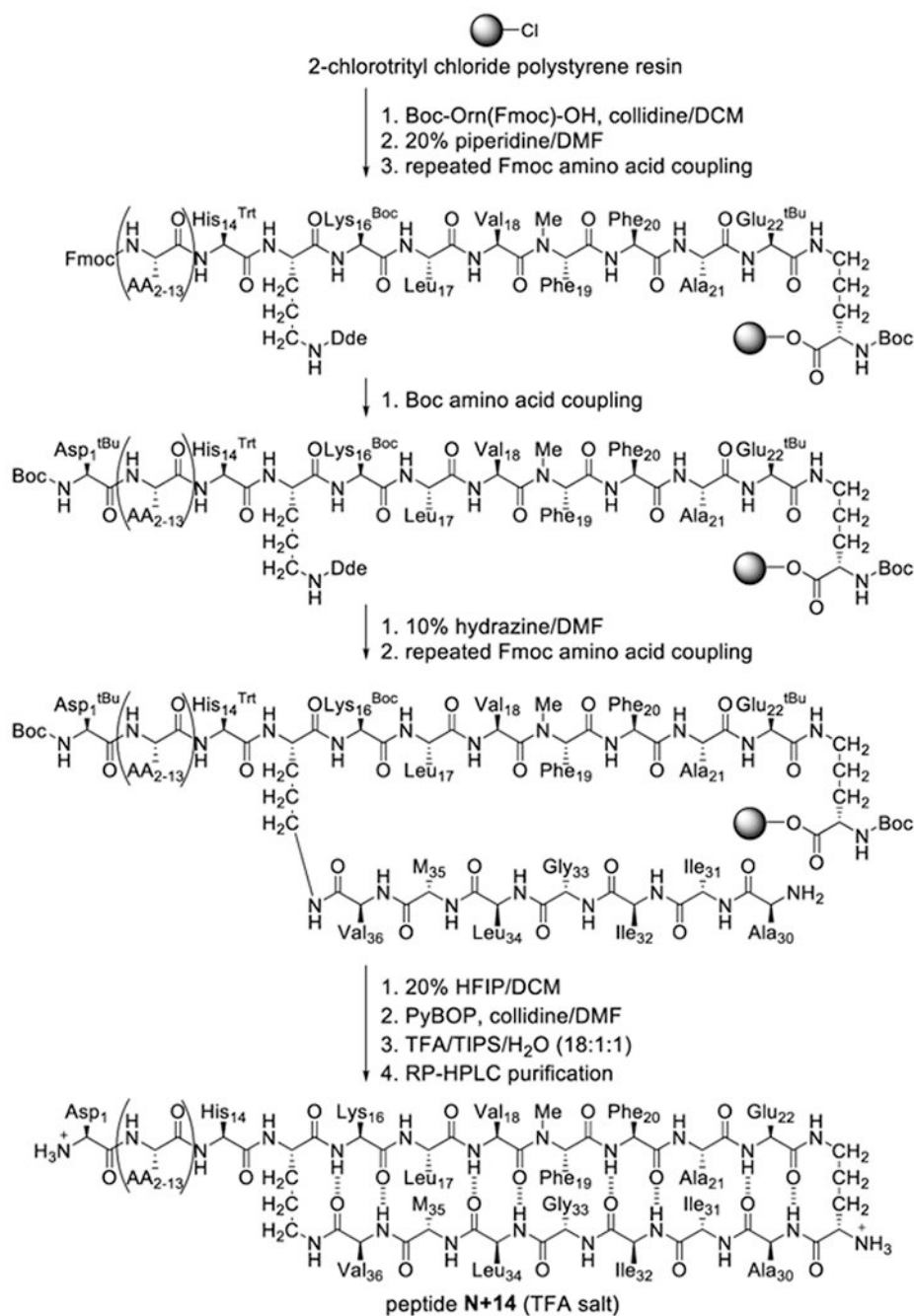


**Figure 2.** Synthesis of the *N*-terminally extended peptide, **N+14** derived from A $\beta$ <sub>1-36</sub>.

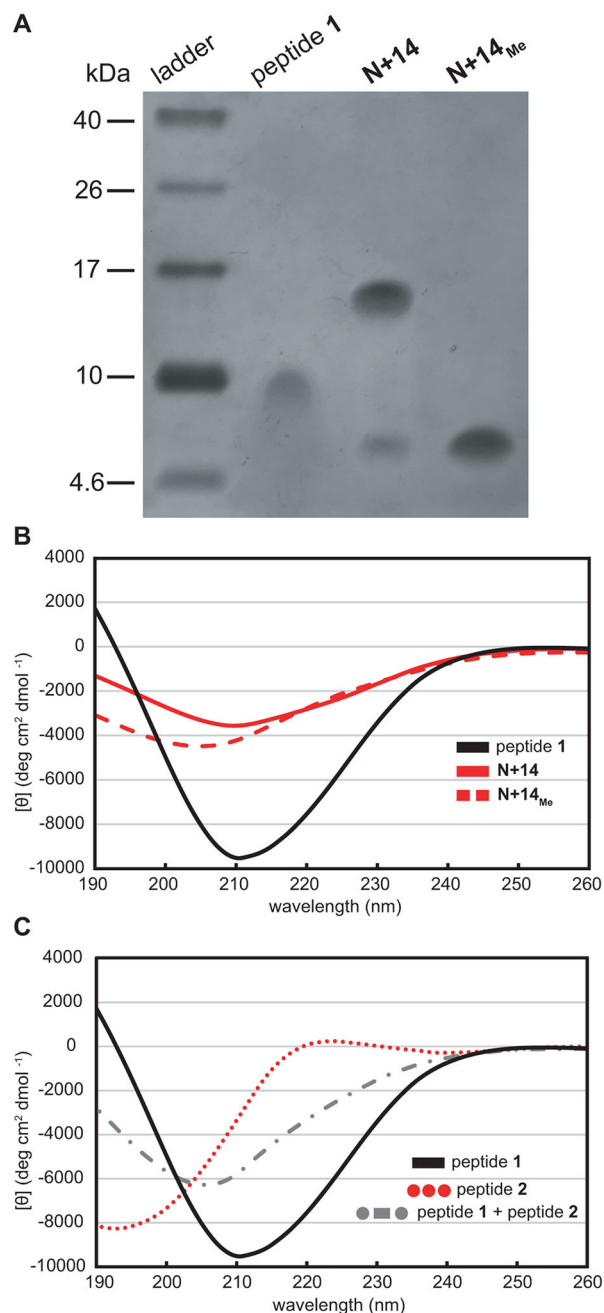


**Figure 3.**

(A) Silver stained SDS-PAGE of peptides **1**, **N+14**, and **N+14<sub>Me</sub>**. SDS-PAGE was performed in Tris buffer at pH 6.8 with 2% (w/v) SDS on a 16% polyacrylamide gel with 75  $\mu$ M solutions of peptide in each lane. (B) Circular dichroism (CD) spectra of peptides **1**, **2**, and an equimolar mixture of peptides **1** and **2**. CD spectra were acquired for each peptide at 50  $\mu$ M in 10 mM phosphate buffer at pH 7.4; the ellipticity was normalized for the number of residues in each peptide.

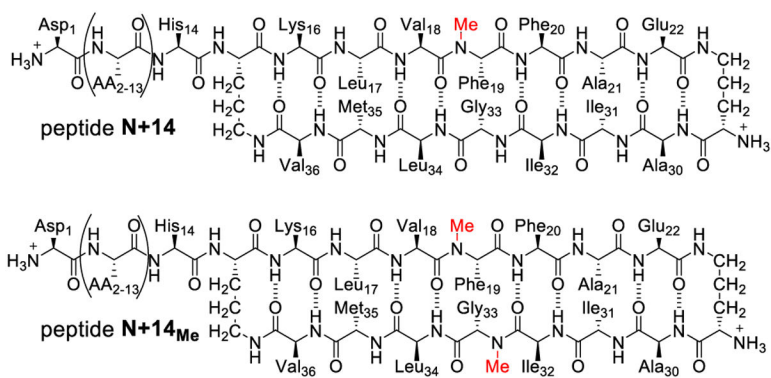


**Figure 4.** Peptide N+14<sub>Me</sub> is a homologue of peptide N+14 with an additional *N*-methyl group on Gly<sub>33</sub> to block hexamer formation.

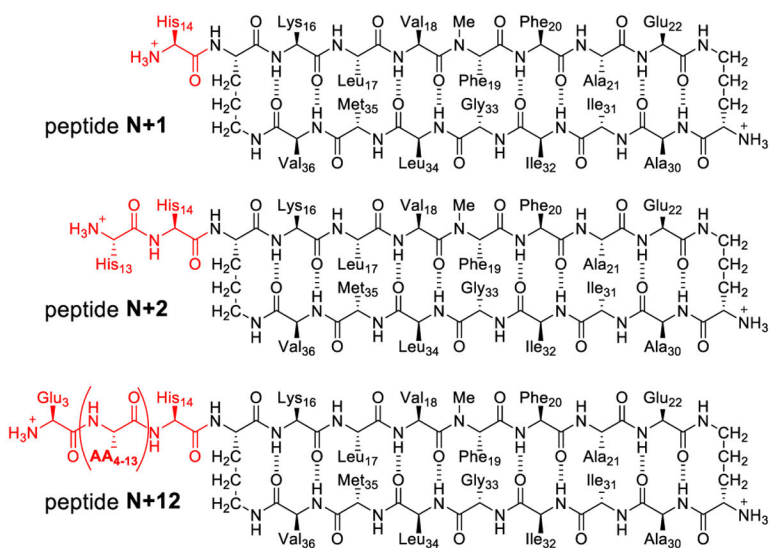


**Figure 5.**  
Peptides N+1, N+2, N+4, N+6, N+8, N+10, and N+12 are homologues of peptide N+14 with truncated tails.

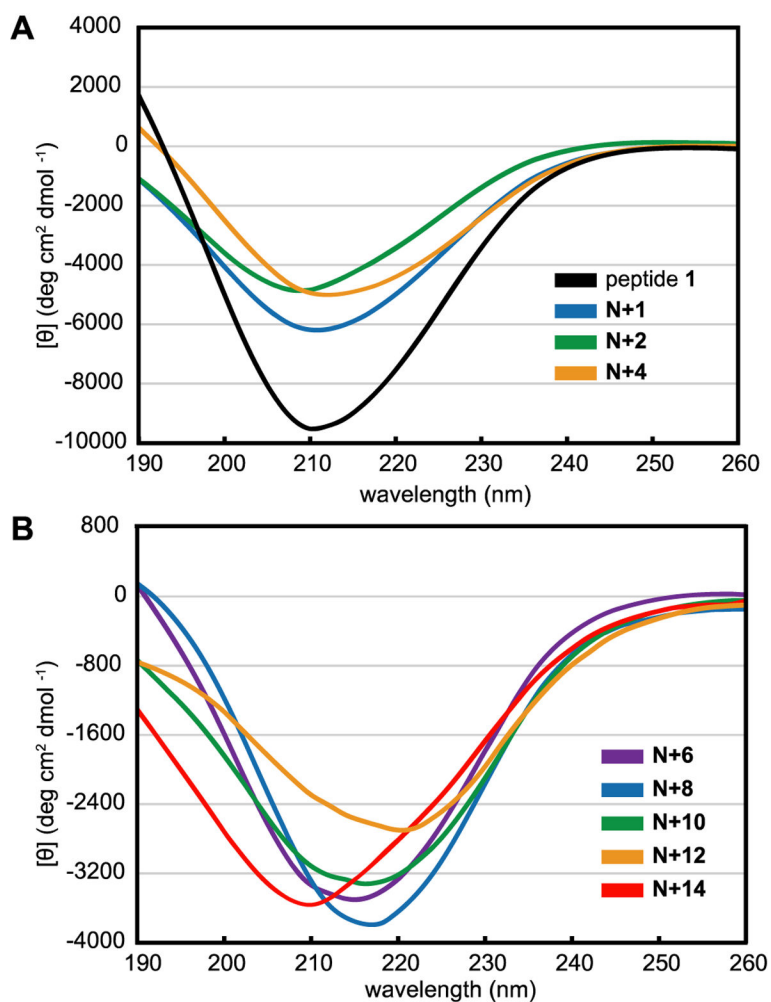


**Figure 6.** CD spectra of peptides **1** and **N+1** through **N+14**. CD spectra were acquired for each peptide at 50  $\mu$ M in 10 mM phosphate buffer at pH 7.4; ellipticity was normalized for the number of residues in each peptide.

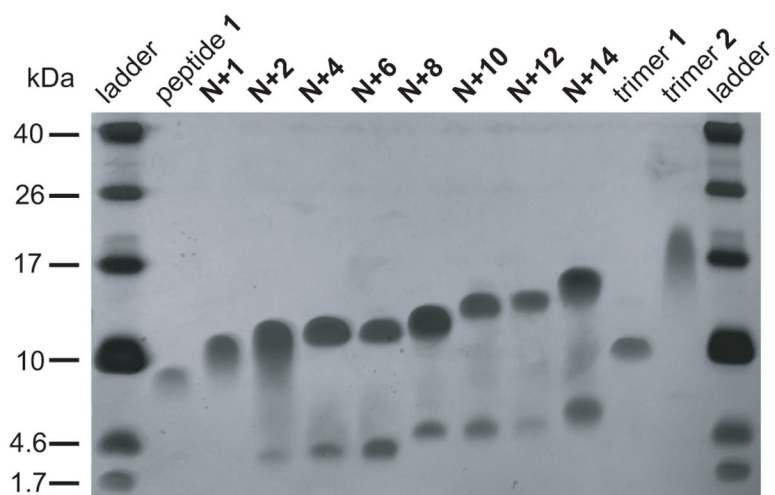


**Figure 7.** Silver stained SDS-PAGE and folding of peptide **1**, peptides **N+1** through **N+14**, and trimers **1** and **2**. SDS-PAGE was performed in Tris buffer at pH 6.8 with 2% (w/v) SDS on a 16% polyacrylamide gel with 75  $\mu$ M solutions of peptide in each lane.

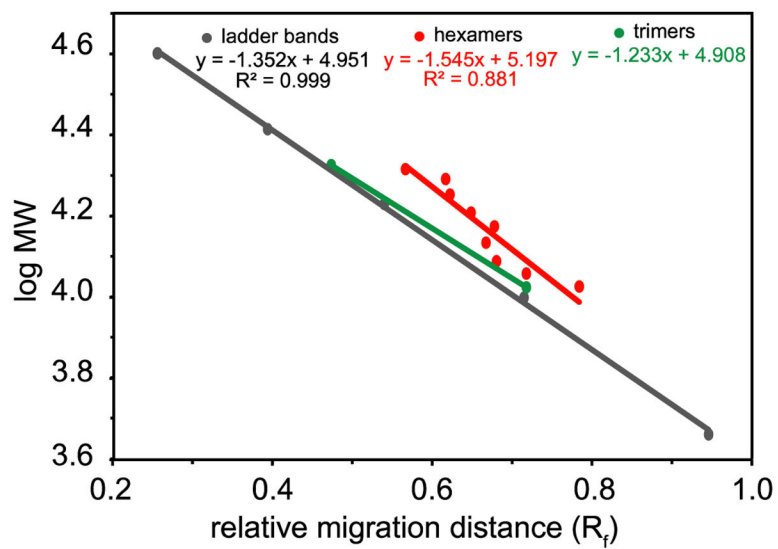


**Figure 8.** Oligomer molecular weights vs. relative migration distance ( $R_f$ ) of peptide **1** and peptides **N** +**1** through **N**+**14** by SDS-PAGE (semi-log plot).

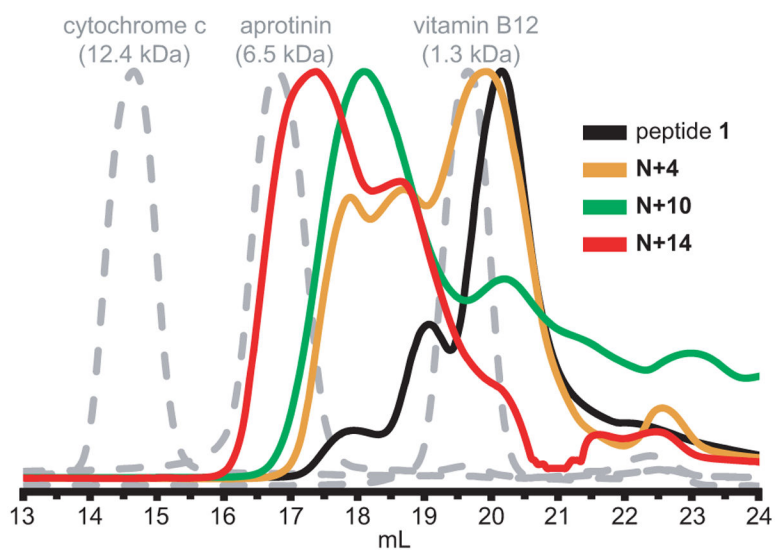


**Figure 9.** SEC traces of peptide **1** and select *N*-terminally extended peptides. SEC was performed on a 1.0 mg/mL solution of each peptide in 50 mM Tris buffer at pH 7.4 with 150 mM NaCl on a Superdex 75 Increase 10/300 column.

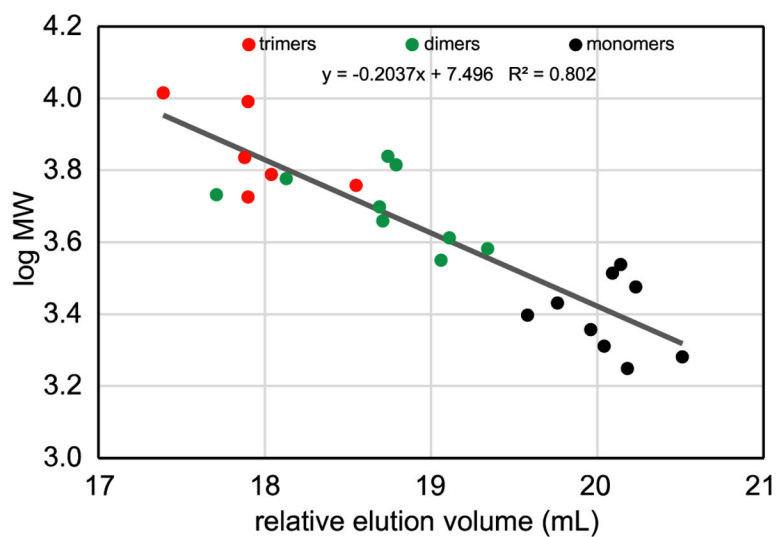


**Figure 10.** Oligomer molecular weights vs. elution volumes of peptide **1** and peptides **N+1** through **N+14** by SEC (semi-log plot). Elution values and oligomer molecular weight are summarized in Supplementary Table 2.

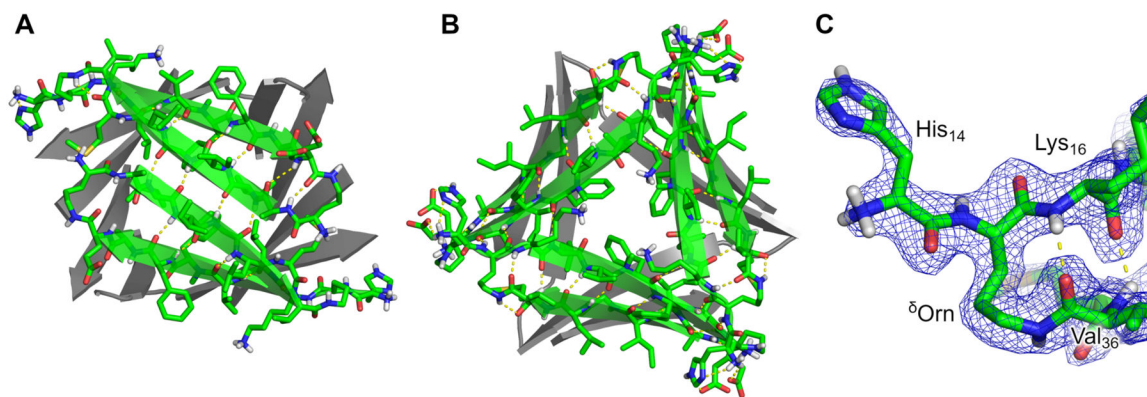


**Figure 11.** X-ray crystallographic structure of the hexamer formed by peptide **N+1** (PDB 6VU4). (A) The trimer subunit within the X-ray crystallographic structure of the hexamer formed by peptide **N+1**. (B) The dimer subunit. (C)  $2F_o - F_c$  electron density map contoured at  $1.3\sigma$ , showing His<sub>14</sub> in peptide **N+1**.  $R_{\text{work}}$ : 0.22,  $R_{\text{free}}$ : 0.26, PDB 6VU4.